Applied Catalysis B: Environmental 147 (2014) 965–972

Contents lists available at ScienceDirect

Applied Catalysis B: Environmental

journal homepage: www.elsevier.com/locate/apcatb

Regenerable cerium oxide based odor adsorber for indoor air purification from acidic volatile organic compounds

R.A. Raso, A. Stepuk, D. Mohn, D. Paunescu, F.M. Koehler, W.J. Stark*

Institute for Chemical and Bioengineering, Department of Chemistry and Applied Biosciences, ETH Zurich, 8093 Zurich, Switzerland

ARTICLE INFO

Article history:
Received 2 July 2013
Received in revised form 9 October 2013
Accepted 11 October 2013
Available online 19 October 2013

Keywords:
Catalytic oxidation
Odor reduction
VOC
Active carbon
Sustainable

ABSTRACT

Indoor odor management currently relies on energy-intensive high air exchange rates, or, more sustainable, on single use volatile organic compounds (VOC) adsorbers or ozonisation. This study investigates a more sustainable, multi-cycle use of an odor adsorber system that combines concepts from catalytic oxidation and air cleaning. Both pure and sodium doped, nanostructured CeO_2 were tested as adsorber material for high volume removal of odorous compounds from air. As a representative compound for unpleasant odors, hexanoic acid (HA) was used. After air cleaning on fixed beds of CeO_2 or Na/CeO_2, both hexanoic acid loaded adsorber materials were heated under air and displayed considerable oxidation activity at 191 °C and 263 °C, respectively. Mass spectroscopy was used to confirm that no hexanoic acid desorbed during combustion. Cerium oxide showed an adsorber efficiency of ≥96.5% over a period of 60 h (C_{in} = 0.044 mg/L, gas hourly space velocity, GHSV = 440 h^{-1}) and sodium doped cerium oxide adsorbed ≥97% for over 90 h (C_{in} = 0.056 mg/L, GHSV = 1100 h^{-1}). CeO_2 was regenerated at 220 °C in air and could be successfully re-used as adsorber without noticeable loss in performance. The study demonstrates that CeO_2 has most promising properties for application as re-usable air cleaner due to its very good ability for adsorption even at highly dilute conditions (ppm-level) using a representative acidic test compound with rancid and sweaty odor. Sodium as a basic dopant further improved the adsorption of hexanoic acid but requires a higher regeneration temperature.

1. Introduction

Reduction of unpleasant odors deriving from volatile organic compounds (VOC) is an urgent need in domestic-, industrial areas and in public transportation. Commonly used strategies for removal of VOC today consist in air exchange, adsorption on activated carbon [1–3] or photo oxidation [4–7]. Unfortunately, all treatments are of considerable energy demand [4,5], depend on regular and cost-intensive replacement and maintenance, or can produce dangerous side products [8,9]. When air is simply exchanged, polluted air is usually replaced by fresh air from outside. This procedure requires high volume exchange rates (typically three times the room volume each hour). The air then has to be heated up or cooled, and optionally filtered as it often contains particulate matter (e.g. soot/fine dust from car engines or flue gases). Modern air standards require for every ventilation or air conditioning system removal of particulate material [10,11]. This results in huge energy consumption from air circulation (pressure drop) and cooling or heating (latent heat; 1.2 kJ/m^3 and °C temperature difference). More sustainable forms of air purification are needed and should provide alternatives to reduce the massive air exchange and hence heat transfer. Air purifiers usually adsorb unpleasant odors and small particles by simple air circulation through an adsorber unit, typically based on active carbon (adsorption of VOC, smelling compounds) and HEPA (high efficiency particulate air) filters. A significant drawback comes from the necessity to periodically replace adsorber units when their capacity is exhausted [1] since such replacement usually needs working personnel to drive to a site of application and manually install a new unit. Therefore adsorber regeneration on site would help to reduce maintenance intervals and costs. New systems additionally use titanium oxide (TiO_2) and UV light to adsorb and remove odor by photo oxidation [4–7]. This prolongs the adsorber's lifetime. Continuous UV light generation, however, consumes considerable amounts of energy. More recently, nano-confined catalytic oxidation (NCCO, ozone treatment of air in zeolites pores), has emerged as a valuable alternative to conventional air purification systems [12].

Unpleasant odors usually consist of volatile organic molecules from several chemical classes like fatty acids, lactones, aldehydes, ketones, heterocyles, phenols and sulphur containing molecules. Most of these substances are easily adsorbed on activated

* Corresponding author. Tel.: +41 44 6320980; fax: +41 44 6331083.
E-mail address: wendelin.stark@chem.ethz.ch (W.J. Stark).

0926-3373/$ – see front matter © 2013 Elsevier B.V. All rights reserved.
http://dx.doi.org/10.1016/j.apcatb.2013.10.030

carbon at ambient temperature and pressure [1–3]. As alternatives to activated carbon for air purification, a number of metal oxide nanoparticles, such as MgO, CaO or Al_2O_3, have been investigated [13]. The removal of halogenated compounds out of air by destructive adsorption on nanoscale oxides has been investigated by Volodin et al. [14]. A well-studied and widely used metal oxide in industrial oxidation catalysis and in air purification is cerium oxide (CeO_2) [15]. Its excellent catalytic properties have been reviewed by Trovarelli [16]. More detailed, when CeO_2 acts as an oxidizing agent it is reduced to CeO_{2-x} and defects containing Ce^{3+} are formed. It is generally agreed that the main compensating defects in CeO_{2-x} are oxygen vacancies [17]. This non-stoichiometry is possible because cerium is able to change its oxidation state rapidly allowing the reversible addition and removal of oxygen, making CeO_2 an oxygen storage material for oxidation reactions. It has been shown for the oxidation of CO that the oxygen atom needed comes from ceria. It is expected that this process involves creation of an oxygen vacancy on ceria leaving a positive charge that is compensated by reduction of cerium [18]. The role of defects enhancing heterogeneous catalytic activity of ceria is accepted but is still an active area of research [19]. Oxygen vacancies defects (OVD) sites have shown to be very important in the oxidation processes e.g. for CO [20,21]. The enhanced activity can be attributed to the oxygen storage capacity (OSC) of ceria which is linked to the ease of cerium to change oxidation states as mentioned before [19]. We assume that similar aspects play an important role in the oxidation of acidic VOC as described in this work.

Since the 1980s, ceria has been used in three-way catalyst (TWC) for the abatement of hydrocarbons, carbon monoxide and nitrogen oxides (NO_x) out of automotive exhausts [21]. Ceria based catalysts have also been extensively investigated for the removals of volatile organic compounds, optionally after doping with noble metals (e.g. gold) [22] or as mixed metal oxides [23,24]. Continuous catalytic oxidation, however, would require heating an indoor air volume to about 150 °C, which is unpractical. As current benchmark, air conditioning requires about 10–20 W/m^3 (10 K temperature difference) and UV light generation about 0.5–1 W/m^3 room, respectively. Here, we propose to combine the beneficial properties of oxidation catalysis (clean conversion of most acidic VOC to CO_2 and water) with adsorber systems (no heating/cooling costs) through the use of regenerable adsorbers with oxidative properties. As test compound we used hexanoic acid. This compound is present in exhaled breath in a concentration of 10 ppbv [25]. Additionally, this compound meets the requirements for our study as HA has a penetrant odor. As small acidic compound, it is representative for other small acidic VOC found in human breath or sweat like propanoic acid, butyric acid, isobutyl acid, valeric acid and isovaleric acid [26,27].

2. Experimental

2.1. Cerium oxide particle based fixed bed adsorber systems

Cerium oxide (CeO_2) (15–30 nm APS, 99.5% purity, 30–50 m^2/g SSA) was purchased from Nanostructured & Amorphous Materials Inc. Texas, USA and used as received. *Sodium doped cerium oxide (Na/CeO_2)* was prepared by incipient wetness impregnation: A mixture of CeO_2 and sodium carbonate (9.3 wt% with respect to CeO_2; Merck, EMSURE ISO) was produced by adding a 2.5 wt% solution of Na_2CO_3 in water to cerium oxide. The humidity of the mixture was adjusted with additional water to produce a granular, homogeneous material. The mixture was allowed to mature over night at 120 °C in air and was calcined in air at 500 °C for 30 min to yield sodium doped CeO_2.

2.2. Adsorber material characterization

Both adsorber materials CeO_2 and Na/CeO_2 were loaded with hexanoic acid (HA, Aldrich, 99%) by first preparing a HA solution in hexane or diethylether, then impregnating the material and drying it under reduced pressure (removal of the solvents) in order to get a final loading of up to 5 wt% HA on CeO_2. *Thermogravimetry* (TG) analysis (Linseis TG/STA-PT1600) was performed under air (6 L/h) from 20 °C to 600 °C with a heating rate of 10 °C/min. The gas stream from the instrument was analyzed with a mass spectrometry (MS) system (OmniStar^{TM} GSD 320, 60 eV, 1–100 amu, 0.1 s/amu scan time) to identify decomposition products from HA oxidation on the cerium oxide, or desorbed HA itself. The specific surface area (SSA) was determined on a Tristar Micromeritics (Norcross, GA, USA) using the Brunauer–Emmett–Teller (BET) method at 77 K [28]. *X-ray diffraction* (XRD) patterns were recorded on an X'Pert PRO–MPD diffractometer (Cu-$K\alpha$) radiation, X'Celerator linear detector system; PANalytical, the Netherlands) with a step size of 0.033 [28]. The particle size distribution of CeO_2 was measured using a Lumisizer 6102-83 (12 channels, λ = 470 nm, 4000 rpm). A stable dispersion was prepared by mixing 1 wt% CeO_2 particles, 0.1 wt% 2-[2-(methoxyethoxy)ethoxy]acetic acid (TODS, Aldrich, technical grade), in ethanol (technical grade) and zircon oxide (0.2 mm) spheres. A ball mill (Fritsch pulverisette 7, premium line) was used for production of the dispersion that was used for above mentioned particle size distribution analysis. Diffuse reflectance infrared Fourier transform spectroscopy (DRIFTS) analysis was performed on a Tensor 27 (Bruker) spectrometer equipped with a PIKE DiffuseIR accessory. Spectra were collected from 4000 to 400 cm^{-1} (256 scans) using a 10 wt% KBr mixture.

2.3. Adsorber performance tests

Loading of hexanoic acid on the fixed bed was achieved by flushing artificial contaminated air (1.02 m^3/day) over the fixed bed adsorber. The contaminated air was prepared by passing compressed air through a gas washing bottle containing liquid HA and equipped with a glass sintered bottom to ensure that all air bubbles had sufficient contact with the HA for saturation. This air stream was then directed on a fixed bed consisting of CeO_2 particles (bed height: 10.5 cm; diameter: 3.5 cm) or Na/CeO_2 particles (4 cm height; same bed mass as for CeO_2, but the sodium doping affords a higher powder packaging density). Potential transportation of entrained HA droplets onto the fixed bed was avoided by inserting glass wool in the upper part of the saturation bottle into the airstream. Use of an upwards mounted tube to transport the HA loaded air further allowed accidentally formed droplets to condense on the walls and flow backwards. Absence of significant droplet entrainment could further be excluded based on the fact that the here experimentally observed HA gas concentrations are in the range of what is thermodynamically expected. The inlet HA concentration was measured at the starting point of the fixed bed before loading (see Fig. 1) and the outlet concentration was measured after different adsorption times. All sampling was done at room temperature and environmental pressure, and made use of standard air quality testing protocols (2-step procedure: First, the sample is collected on an adsorber tube, then desorbed and analyzed by gas chromatography). Samples were collected using commercial silica gel adsorber tubes (Dräger Typ-G) for acidic VOC and a standardized, calibrated pump (Dräger X-act 5000) using a standard pump rate of 0.5 L/min and sampling times from 15 to 240 min depending on the targeted detection limits. Desorption of the collected hexanoic acid was done by washing the silica gel with 5.0 mL methanol (EMSURE, ISO Reag.) and further analyzing the extract by GC-FID (Agilent GC 6890, average error ±10%) as directed by the manufacturer. The "used" fixed bed was removed from the

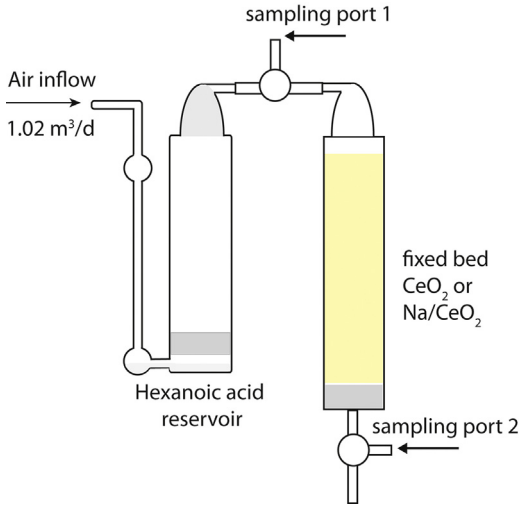

Fig. 1. Experimental setup to add a representative model compound for sweaty/rancid odors into an indoor air stream consisting of a reservoir containing hexanoic acid (left) and fixed bed (right). Air (1 m^3/day) is flushed through the liquid and carries gaseous hexanoic acid to the fixed bed. The transport of aerosols is impeded by a glass wool filter on top of the reservoir.

saturation setup (Fig. 1) and transferred into a tubular oven for regeneration tests (Fig. 2).

The adsorber part of the experimental setup is operated in two modes: In the "air cleaner" mode, the acidic organic volatile compounds are adsorbed at room temperature onto the fixed bed (see Fig. 2). When adsorption was complete (starting breakthrough of HA as detectable qualitatively by smelling or quantitatively using gas chromatography), the fixed bed adsorber was heated up to 220 °C in the case of CeO_2. During this period, the adsorbed organic volatiles are catalytically oxidized to CO_2 and water. Since the system remained open for the whole process, enough oxygen was available to oxidize the contaminant. After cooling to room temperature, the CeO_2 fixed bed adsorber was used again for a next "air cleaning" cycle.

2.4. Preliminary olfactory tests

Preliminary olfactory tests were carried out on CeO_2 and Na/CeO_2 loaded with 5 wt% hexanoic acid respectively. Half of the material was heated up to 220 °C for 15 min in a furnace and the other half was kept at ambient temperature. Six volunteers (two females and four males) were selected. All informed volunteers were free of acute respiratory disease like nasal track infections,

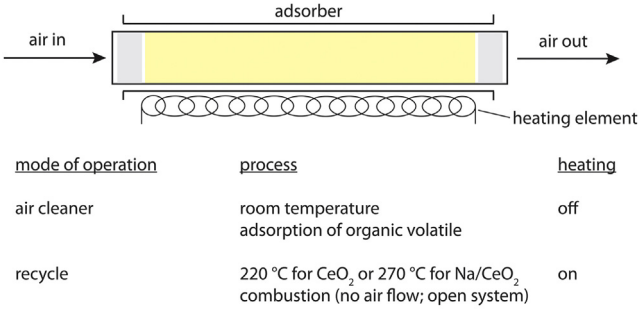

Fig. 2. Cerium oxide based adsorbers can be operated in two modes: As air cleaners, volatile compounds adsorb from ambient air, the heating is off. During regeneration, the adsorber (open system) is heated up for a short time, resulting in oxidation of the adsorbed compounds, release of carbon dioxide and water, and returning a functional adsorber. The system is then ready for a next (usually multiple hours to days) period of air cleaning.

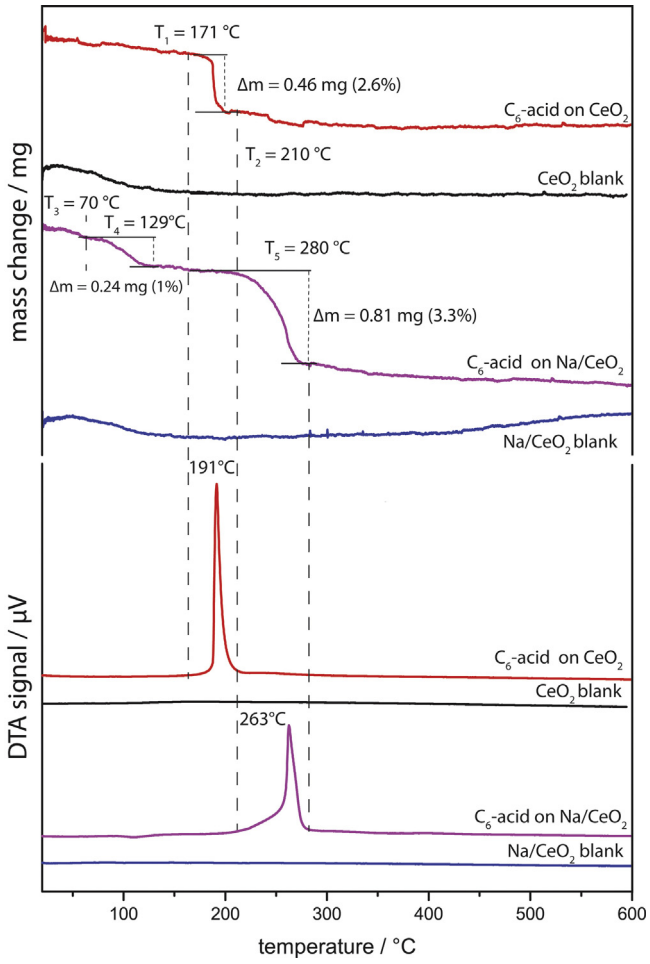

Fig. 3. Thermogravimetric analysis (TG–DTA) of hexanoic acid (C_6-acid) loaded on CeO_2 and sodium-doped cerium oxide (Na/CeO_2). Decomposition occurs at very mild conditions, well below 300 °C, and is characterized by appearance of a rather sharp mass loss. Sodium doping delayed the catalytic oxidation activity of the cerium oxide support by about 70 °C.

sinusitis or rhinitis. The test was performed in a well-ventilated room at 22 °C. Samples were located in ceramic vessels with 25 mm in diameter and filled to one third (volume). Study participant were asked to inhale from about 4 cm distance the air above the samples and assign a value from 1 to 6 (1 no intensity, 6 very high intensity) according to their subjective olfactory perception.

3. Results and discussion

3.1. Catalytic activity

In order to investigate the possibility for clean regeneration, we carried out a number of preliminary experiments on the catalytic combustion of hexanoic acid on cerium oxide using a TG-DTA–MS system. The thermobalance was loaded with different samples of HA on CeO_2 or Na/CeO_2 nanoparticles and heated up as described in 2.2. For HA on CeO_2 catalytic combustion was observed between 171 °C and 210 °C with a peak at 191 °C corresponding to the maximum mass change rate and maximum reaction enthalpy. In contrast, doping with sodium delayed the decomposition activity. HA on Na/CeO_2 showed a mass loss corresponding to the decomposition of hexanoic acid between 210 °C and 280 °C with a maximum at 263 °C (see Fig. 3). A second, minor mass change observed between 70 °C and 130 °C derives from the release of water and carbon dioxide probably originating from carbonic acid

(chemisorbed CO_2, adsorbed water, see mass spectroscopy pattern in Fig. 4). These results show the ability of CeO_2 and Na/CeO_2 to decompose hexanoic acid at comparatively low temperatures. In contrast to non-catalytic oxidation, or combustion-assisted VOC decomposition (usually at 600–1200 °C), the here used temperatures are amenable for device manufacturing.

Mass spectra recorded during catalytic decomposition runs clearly showed the predominant formation of carbon dioxide and water. Trace amounts of hydrogen (m/z 2) were formed for HA on pure, non-doped CeO_2 compared to HA on Na/CeO_2 and suggests a minor contribution from a cracking type process on the surface of the catalyst. Next to these three main components, traces of a range of lower molecular mass ions were found in the gas stream (from ionization or fragmentation in ion source) suggesting some side product formation during catalytic combustion. From the absence of two main ions (m/z 60 and 73 characteristic for intact hexanoic acid, see Fig. 4, right) in catalytic oxidation test runs, however, we can conclude that no hexanoic acid desorbed as an intact molecule and escaped the cerium oxide matrix. Note that HA produces a characteristic set of molecular ions when fed into the MS. These peaks are absent in the cerium oxide–catalyzed decomposition samples. The additional m/z found can be attributed to lower molecular mass derivatives of hexanoic acid such as 1-pentene, 2-pentene (*cis*/*trans*; both m/z 70), both typical cracking process side products. The observation of traces of hydrogen (s. above) would further be in line with a minor contribution from cracking. According to MS spectra, different processes are taking place on CeO_2 if compared to sodium-doped adsorbers based on Na/CeO_2. The main differences are visible for hydrogen (m/z 2) and pentene (m/z 70, stronger on CeO_2). The main oxidation (i.e. formation of water/CO_2) happens in two stages on Na/CeO_2. The first water/CO_2 release is not accompagnied by the typcial oxidation by-products (see MS traces) and probably originates from the decomposition of carbonates and dehydration. This is not surprising, given the basic properties of sodium (formation of hydrogen carbonates and carbonates) and the hygroscopic nature of the associated sodium species (both sodium hydroxide and carbonates are very hygroscopic). These compounds also form multiple hydrates (e.g. Na_2CO_3 10 H_2O) that decompose in this temperature window.

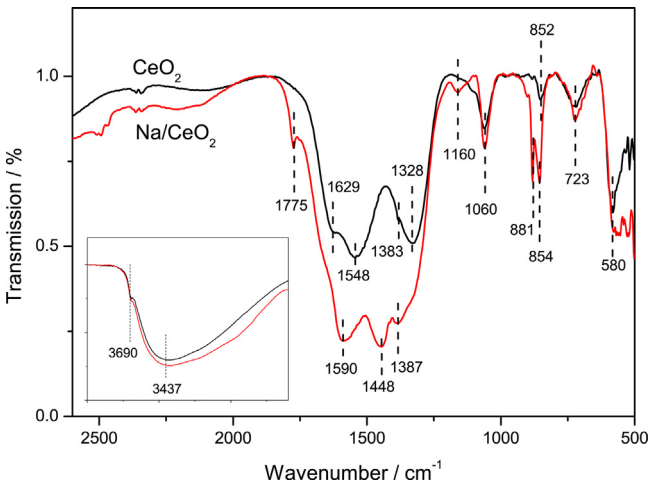

Fig. 5. DRIFTS spectra of CeO_2 (black) and Na/CeO_2 (red). (For interpretation of the references to color in this figure legend, the reader is referred to the web version of this article.)

These findings are supported by DRIFTS analysis which revealed the presence of carbonates on CeO_2 and Na/CeO_2. Results are summarized in Fig. 5 and Table 1. Major differences from these samples are represented by signals at 1775, 1590, 1448, 1387, 1160 and 881 cm^{-1} which are less pronounced or absent on untreated ceria. Carbonates found on CeO_2 are likely to arise from chemisorption of carbon dioxide from air [29] whereas carbonates found on Na/CeO_2 are likely to be a combination of chemisorbed CO_2 and residual carbonates originating from treatment with sodium carbonate. In addition, during calcination, sodium oxide is likely to be formed by releasing CO_2 [30] well below decomposition temperature (800 °C [31]). Hence, signals found at 1775, 1448, 1387. 1160 and 881 cm^{-1} are attributed to sodium oxide (SDBS database: 1776, 1453, 1378, 1180 and 879 cm^{-1}). The signal found at 1590 cm^{-1} may indicate the reduced state of ceria surface for Na/CeO_2 as indicated by Binet et al. [32].

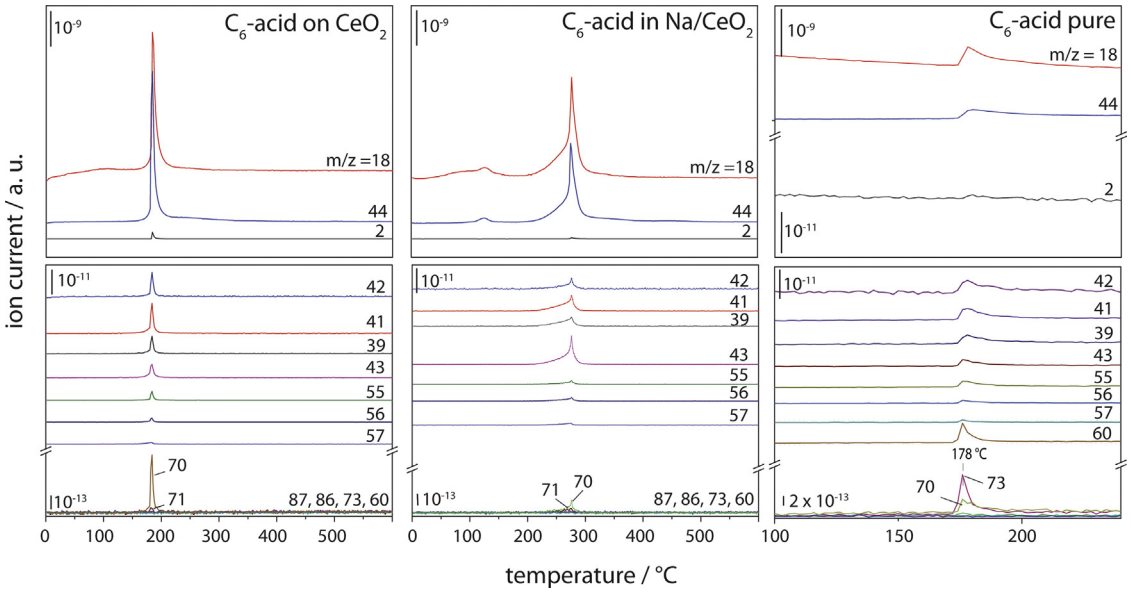

Fig. 4. Mass spectroscopic analysis of combustion off-gas from thermal decomposition of hexanoic acid (C_6-acid) as vapor (right) and after adsorption on CeO_2 and Na/CeO_2. For HA on CeO_2 formation of cracking by-products such as pentene isomers (m/z 70) are observed. Sodium doping alters the MS spectra and results in an early water and CO_2 peak associated with hydrates and carbonate decomposition.

Table 1
DRIFTS signal assignment for CeO_2 and Na/CeO_2.

CeO_2 [cm^{-1}]	Assignment	Ref.	Na/CeO_2 [cm^{-1}]	Assignment	Ref.
3690 (3695)	ν(OH), surface adsorbed water	[29,33,34]	3690 (3695)	ν(OH)	[29,33,34]
3437 (3435)	ν(OH), H-bonded water	[33,35]	3437 (3435)	ν(OH), H-bonded water	[33,35]
1629 (1630, 1628)	Surface adsorbed water, carboxylate	[29,36]	1775 (1795)	Na_2O, (Na_2CO_3)	[37]
1548 (1553)	Carbonate[a]	[29]	1590[b] (1587)	bi-dentate carbonate	[32]
1383 (1382)	$\nu(CO_3)$, core carbonate	[33]	1448 (1453,1450)	Na_2O, Na_2CO_3	[37]
1328 (1344)	Carbonate	[34]	1387 (1378, 1396)	Na_2O, HCO_3^-, $\nu(CO_3)$ core carbonate	[33,34]
1060 (1070)	ν_s(OCO), CO_2^{2-}	[33]	1160 (1180, 1150)	Na_2O, ν_s(OCO), CO_2^{2-}	[32]
852 (860, 851)	Polydentate carbonate, $\pi(CO_3)$, carbonate[a]	[29,32,33]	1060 (1070)	ν_s(OCO), CO_2^{2-}	[33]
723 (730)	ν(CeO) fundamental	[33]	881	Na_2CO_3	[37]
			854 (860, 851)	polydentate carbonate, $\pi(CO_3)$, carbonate[a]	[29,32]
			723 (730)	ν(CeO) fundamental	[33]

( ) Wavenumber in parenthesis are values found in literature.
[a] Chemisorbed CO_2 from air [29].
[b] Reduced state of ceria surface [32].

The oxidation peak is very sharp on CeO_2 (lasting about 20 °C, presumably indicating a light-off phenomenon) while it is prolonged on Na/CeO_2 (lasting about 70 °C) as seen in Figs. 3 and 4. In summary, from thermogravimetry analysis the working temperature is estimated to be situated for CeO_2 between 171 °C and 210 °C and for Na/CeO_2 between 210 °C and 280 °C. Average turnover numbers are found to be for CeO_2 $TON_{171\,°C\text{-}210\,°C} = 0.96\ \mu mol/(g\,s)$ and for Na/CeO_2 $TON_{210\,°C\text{-}280\,°C} = 0.70\ \mu mol/(g\,s)$. These values are comparable to values found in the literature [38,39].

3.2. Regenerable CeO_2-based adsorber performance

The outlet concentration of hexanoic acid after passage over the cerium oxide based fixed bed confirmed a high affinity of the adsorber material for the volatile, HA (Fig. 6, Table 2). The off–gas remained nearly odorless for a prolonged time (adsorber fully working) and then subsequently allowed HA to slip through. For cerium oxide, the experiment was carried out using three different inlet concentrations. From data collected it can be seen that for about 50 h no hexanoic acid (below limit of detection, LOD) breaks through the CeO_2 bed when using an inlet concentration of about 0.044 mg/L (clearly identified as "strongly smelling" by humans) and a gas hourly space velocity (GHSV) of 440 h^{-1}. After that, a maximum outlet concentration (break through) is measured at about 70 h followed by a slight decrease in concentration up to 170 h after starting the adsorption process (see Fig. 6). The minor decrease in concentration after breakthrough of HA may be a result of starting autoxidation of the hexanoic acid in the reservoir, or through bed restructuring. A second test run used a hexanoic acid inlet concentration of 0.028 mg/L and samples were taken up to 240 h after start (a longer experiment at lower inlet concentration than in the first experiment). A maximum outlet concentration of 0.015 mg/L was measured after 90 h. After about 10 days, the HA concentration in the outlet had dropped to about 0.011 mg/L. The fixed bed of this second run was regenerated (oxidation of the HA as described in 2.3) and reused as adsorber. In a third run, an initial HA concentration of 0.035 mg/L was applied. After 70 h, again no HA could be detected in the outlet gas stream. After 157 h a concentration of 0.018 mg/L HA was measured indicating breakthrough of the test compound (Fig. 6, green squares). This shows the ability of CeO_2 to adsorb HA out of air and to be regenerated without noticeable loss in performance.

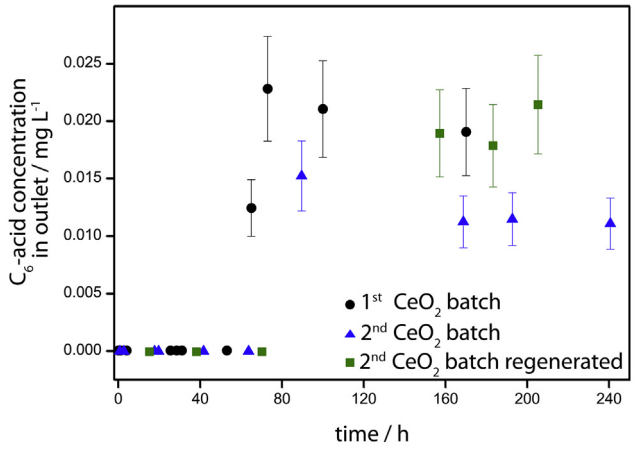

Fig. 6. Adsorption of hexanoic acid at relevant indoor concentrations on CeO_2 based fixed beds. Bed saturation and breakthrough occurred between 53 and 65 h (1st, 1.02 m^3/d, C_{inlet} = 0.044 mg/L) and between 64 and 90 h (2nd, 1.02 m^3/d, C_{inlet} = 0.028 mg/L). A regenerated fixed bed (2nd regenerated, 1.02 m^3/d, C_{inlet} = 0.035 mg/L) again showed no breakthrough up to 70 h and confirmed that regeneration was possible without significant loss of adsorption capacity (average error ±10%). (For interpretation of the references to color in this figure legend, the reader is referred to the web version of this article.)

Sodium doped adsorber Na/CeO_2 was used in a first experiment with a fixed bed height equal to that of pure CeO_2. Due to its higher packaging density, though, about 2.7 times more material was needed to fill the fixed bed volume. This set up was so efficient, that even after 170 h (one week) no hexanoic acid was detected in outlet gas stream at an inlet gas HA concentration of 0.056 mg/L and a gas hourly space velocity (GHSV) of 440 h^{-1} (see Fig. 7). A second experiment with the same mass of adsorber material as the pure cerium oxide was designed (10.0 g adsorber per bed) and resulted in a 4 cm high bed and GHSV of 1100 h^{-1}. Here, for up to 96 h, no breakthrough of the HA was observed suggesting a higher capacity for Na/CeO_2 in adsorbing hexanoic acid than CeO_2, in line with an expected contribution of the alkaline sodium to fix HA as a carboxylic acid salt.

The efficiency of an adsorber can be calculated by following formula:

$$A_{eff} = \frac{C_{in} - C_{out}}{C_{in}}$$

where C_{in} and C_{out} are the inlet and outlet concentrations of hexanoic acid in the gas stream. Where no hexanoic acid was found, the limit of detection (LOD) of the here used chromatography and adsorption based standard analysis method was used. Results are summarized in Table 2. For CeO_2 we measured an about 2 wt% mass increase after breakthrough which corresponds to a surface

Table 2
Adsorber efficiency of cerium oxide based materials.

	First CeO_2 batch	Second CeO_2 batch	Second CeO_2 batch regenerated	First Na/CeO_2 batch	Second Na/CeO_2 batch
Adsorber material [g]	10.0[b]	10.0[b]	10.0[b]	27.0[b]	10.0[c]
C_{in} HA [mg/L]	0.044	0.028	0.035	0.056	0.056
Time, no detection [h]	≥53	≥64	≥70	≥170	≥96
max. A_{eff} [%][a]	96.5	94.6	95.6	97	97

[a] Max. A_{eff} [%] is related to the inlet concentration of HA in the single experiment and refers to the time where no HA has been detected. The limit of detection (LOD) for this method is 1.6 μg/L air (average error ±20%) and A_{eff} [%] gives the minimum value for efficiency related to C_{in} and LOD. However, where no HA was detected this value might be higher.
[b] Fixed bed height was 10.5 cm.
[c] Fixed bed height was 4 cm.

coverage of about 2.5 μmol/m². The mass gain for Na/CeO_2 is a combination of hexanoic acid, humidity and carbon dioxide.

3.3. Preliminary olfactory tests by volunteers

Preliminary human olfactory tests showed that the overall perception of smell over adsorber materials with equal loads of hexanoic acid was stronger on CeO_2 than on Na/CeO_2 (see Fig. 8).

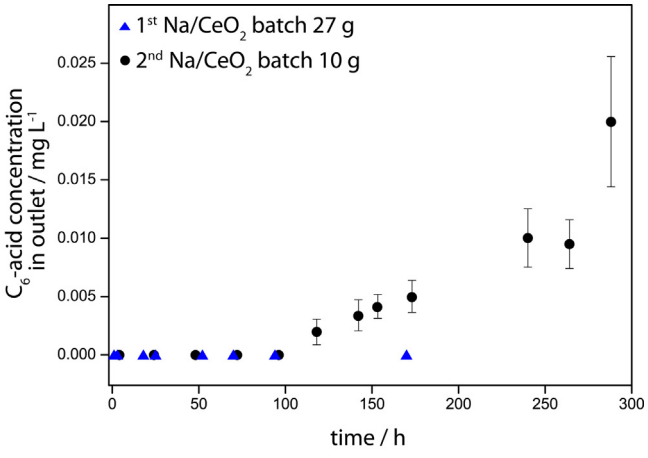

Fig. 7. Sodium doped cerium oxide is an efficient adsorber for hexanoic acid. Up to 170 h (1st run; height of the fixed bed kept constant at 10.5 cm, gas flow of 1.02 m³/d, C_{inlet} = 0.056 mg/L) and to 96 h (2nd run; mass of adsorber kept constant at 10 g per bed, gas flow of 1.02 m³/d, C_{inlet} = 0.056 mg/L) no breakthrough of hexanoic acid was observed (average error ±10%).

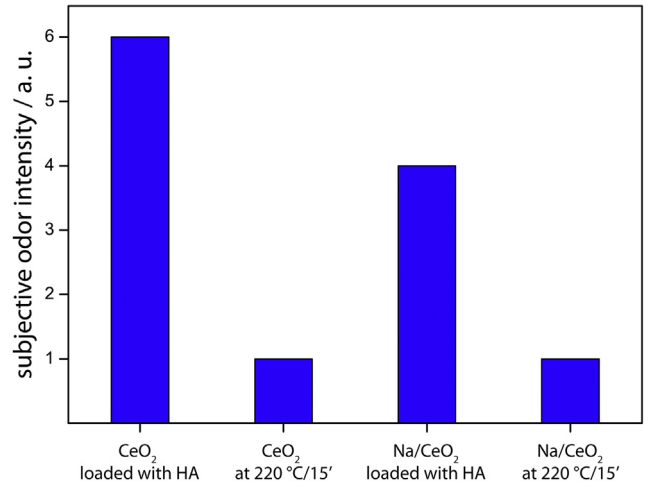

Fig. 8. Preliminary human olfactory tests on CeO_2 and Na/CeO_2 loaded with 5 wt% hexanoic acid before and after temperature treatment at 220 °C. A rating of 6 corresponds to a (subjectively rated and perceived) level of very intense smell whereas 1 was rated as "no smell at all".

This can be explained by a lower partial pressure of hexanoic acid over the carrier material resulting from a stronger binding on the surface. Addition of sodium carbonate as doping agent results in an increased number of adsorption, preferably alkaline centers located on the carrier material. The ability to deprotonate the carboxylic acid of the test compound yields a salt of very low volatility. The formation of the salt species is supported by the observation of an early CO_2 and water release peak in the mass spectrometry analysis (Fig. 4) and the shift of decomposition/oxidation of the HA at higher temperature. After temperature treatment both carrier materials had lost their capability to emit "bad smell".

3.4. Adsorber material characterization

BET analysis showed an increase in particle diameter and a decrease in specific surface area (SSA) when CeO_2 was doped with sodium. After loading the carrier material with HA and heating

Table 3
Specific surface area by nitrogen adsorption at −196 °C of CeO_2 and Na/CeO_2 as prepared and after heating up to 600 °C in air for 1 h. A more pronounced increase in particle size was observed for sodium doped cerium oxide whereas pure cerium oxide remained largely unaffected by this rather low temperature treatment. Nitrogen adsorption analysis.

Sample	S_{BET} [m²/g]	D_{BET} [nm]
CeO_2 as prepared	70.4 to ±3.5	12
Na/CeO_2 as prepared	44 ± 2.2	19
HA on CeO_2/600 °C	61.6 ± 3.1	13
HA on Na/CeO_2/600 °C	21 ± 1	38

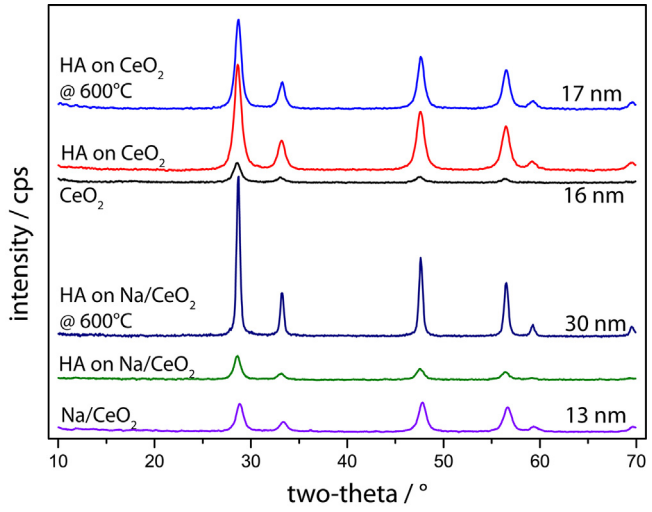

Fig. 9. X-ray diffraction (XRD) confirmed an increase in crystallite size (calculated by Debey–Scherrer equation) of CeO_2 treated with sodium carbonate and heated up to 600 °C for 1 h if compared to untreated CeO_2. Removal of adsorbed HA from CeO_2 at 600 °C and regeneration of the fixed bed adsorber showed a negligible degree of sintering, in agreement with nitrogen adsorption measurements (BET).

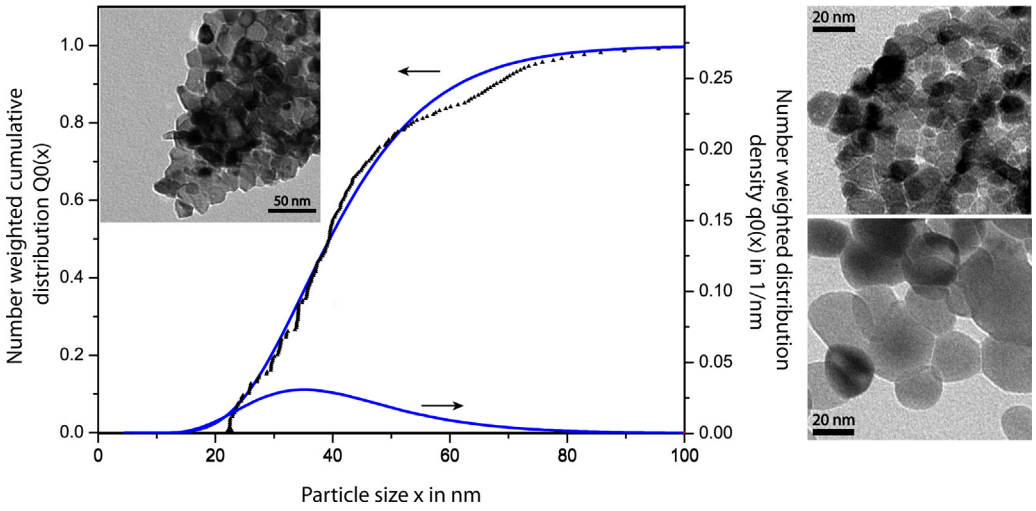

Fig. 10. The particle size distribution as measured in a liquid dispersion and electron micrograph (top left) of CeO_2 as received. 84% of the particles had a hydrodynamic diameter of 59 nm or less with a median situated at 38 nm (blue line: log-normal particle size distribution calculated). Transmission electron micrographs of Na/CeO_2 as prepared (top right) and after heating up to 600 °C in air (bottom right) which affords considerable particle growth due to sintering.

up to 600 °C both materials showed some decrease in SSA (see Table 3). This effect was much more pronounced for sodium doped cerium oxide. In this case sodium acts as melting point lowering agent. Since preparation of Na/CeO_2 involves calcination for 30 min at 500 °C, some particle growth was observed. Even more pronounced sintering was observed for treatment at 600 °C whereas little particle growth was found for pure CeO_2. A similar behavior has been observed by Zotin in temperature programmed reduction of sodium doped ceria [40].

The primary particle diameters were calculated from the SSA according to following formula:

$$D = \frac{6}{SSA \cdot \rho}$$

where D is the primary particle diameter, SSA is the specific surface area and ρ is the density of the material. X-ray diffraction and TEM micrographs (see Figs. 9 and 10) confirmed these SSA derived particle size range.

4. Conclusion

In a model experiment nano-particulate CeO_2 and CeO_2 doped with sodium were tested as adsorber material for the removal of bad smelling volatile compounds out of ambient air. Hexanoic acid (HA) was used as test compound. The catalytic activity, for total oxidation of HA after adsorption, was tested in a TG/DTA for CeO_2 and Na/CeO_2. In air, quantitative combustion was observed on CeO_2 between 171 and 210 °C reaching a peak at 191 °C. On Na/CeO_2 combustion was delayed to higher temperatures at 210 to 280 °C with a peak at 263 °C. From mass spectrometry analysis no desorption of HA was observed. When passing the model indoor air over the adsorber as a fixed bed, cerium oxide could retain ≥96.5% hexanoic acid over a period of 60 h (C_{in} = 0.044 mg/L) and sodium doped cerium oxide reached an efficiency of ≥97% for over 90 h (C_{in} = 0.056 mg/L). Taking into account the different space velocities, namely 440 h^{-1} for CeO_2 and 1100 h^{-1} for Na/CeO_2 a more effective adsorption capacity can be deduced for sodium doped ceria. A full regeneration of the CeO_2 was then performed at 220 °C in air. This material could be reused as adsorber without loss in efficiency. The specific surface area determined for CeO_2 showed a minor decrease from 70 to 62 ± m^2/g upon heating up to 600 °C for 1 h in air. This minor sintering was confirmed by X-ray diffraction analysis and transmission electron micrographs. The origins of catalytic activity of CeO_2 have been discussed in section 1. A possible decrease in activity may arise from (a) loss in surface area or (b) loss of active sites. Surface area loss, as shown in Table 3, was small for CeO_2 upon heating to 600 °C. From this data it can be assumed that regeneration of CeO_2 in a temperature range below 300 °C will not significantly reduce surface area of CeO_2 needed for adsorption and catalytic oxidation. On contrary, the Na supplement has shown to significantly decrease surface area as measured by BET after calcination at 500 °C. A similar behavior has been observed by Zotin in the temperature programmed reduction of sodium doped ceria where BET surface area decreased from 120 m^2/g to 70 m^2/g after treatment at 400 °C [40]. The stability range of sodium supplemented CeO_2 has not yet been completely investigated.

Deactivation may also comprehend loss of oxygen vacancies defects (OVD) and oxygen storage capacity (OSC). Additionally, the supply of oxygen originating from CeO_2 must be ensured. As regeneration happens in an open system well above room temperature, reoxidation of ceria can be assumed to happen during this process. This will restore the initial conditions needed for the next cycle [33,41].

Addition of sodium is expected to generate basic center on the CeO_2 particles. There, the carboxylic acid may be more easily deprotonated and fixed more efficiently on the adsorber. This hypothesis was indeed confirmed as shown by an increased capacity of the adsorber material to capture HA (see TG experiments and a delayed breakthrough of HA in Na-doped ceria (Fig. 7)). The here shown two step batch treatment is more energy efficient compared to continuous oxidation of contaminated air. Since the catalytic combustion of hexanoic acid peaks at around 190 °C, the continuous oxidation would require heating the catalyst at least to that temperature for the whole air cleaning period.

Additionally, the contaminant concentration is expected to be low during that period. Batch treatment, however, removes contaminants at room temperature after first enriching them on the catalyst until a regeneration cycle is required. This lasts for only a fraction of the time compared to continuous oxidation mode which is much more energy efficient.

In summary, CeO_2 showed very promising properties for application as an air cleaner due to its very good ability for adsorbing the representative model compound hexanoic acid out of contaminated air and for its capability for recycling at comparatively low temperature. Na/CeO_2 adsorbed hexanoic acid even stronger than CeO_2 alone but required a higher activation temperature for total

oxidation of the test compound. This work shows the ability of cerium oxide to act as an "on place" regenerable air cleaner adsorber material and hence to substantially reduce energy consumption deriving from conventional air purification systems and room ventilation.

Acknowledgments

Financial support by ETH Zurich is kindly acknowledged. We thank Andreas Dutly and his team for support with gas chromatography.

References

[1] A. Robers, M. Figura, P.H. Thiesen, AIChE J. 51 (2005) 502–510.
[2] P. Pendleton, S.H. Wong, R. Schumann, G. Levay, R. Denoyel, J. Rouquerol, Carbon 35 (1997) 1141–1149.
[3] I.N. Najm, V.L. Snoeyink, B.W. Lykins, J.Q. Adams, J. Am, Water Works Assoc. 83 (1991) 65–76.
[4] C.H. Ao, S.C. Lee, Chem. Eng. Sci. 60 (2005) 103–109.
[5] S. Wang, H.M. Ang, M.O. Tade, Environ. Int. 33 (2007) 694–705.
[6] M.L. Sauer, D.F. Ollis, J. Catal. 149 (1994) 81–91.
[7] H. Yoneyama, T. Torimoto, Catal. Today 58 (2000) 133–140.
[8] Y. Zhang, J. Mo, Y. Li, J. Sundell, P. Wargocki, J. Zhang, J.C. Little, R. Corsi, Q. Deng, M.H.K. Leung, L. Fang, W. Chen, J. Li, Y. Sun, Atmos. Environ. 45 (2011) 4329–4343.
[9] C.J. Weschler, Atmos. Environ. 38 (2004) 5715–5716.
[10] R.D. Brook, J.R. Brook, B. Urch, R. Vincent, S. Rajagopalan, F. Silverman, Circulation 105 (2002) 1534–1536.
[11] S.A. Grinshpun, A. Adhikari, T. Honda, K.Y. Kim, M. Toivola, K.S.R. Rao, T. Reponen, Environ. Sci. Technol. 41 (2007) 606–612.
[12] A. Leung, E. Kwok, Adv. Mater. Res. 550-553 (2012) 607–615.
[13] A. Khaleel, P.N. Kapoor, K.J. Klabunde, Nanostruct. Mater. 11 (1999) 459–468.
[14] A.M. Volodin, A.F. Bedilo, D.S. Heroux, V.I. Zaikovskii, I.V. Mishakov, V.V. Chesnokov, K.J. Klabunde, in: J.P. Blitz, V.M. GunKo (Eds.), Surface Chemistry in Biomedical and Environmental Science, Springer, Berlin, 2006, pp. 403–412.
[15] A. Trovarelli, C. de Leitenburg, M. Boaro, G. Dolcetti, Catal. Today 50 (1999) 353–367.
[16] A. Trovarelli, Catal. Rev. 38 (1996) 439–520.
[17] M. Mogensen, N.M. Sammes, G.A. Tompsett, Solid State Ionics 129 (2000) 63–94.
[18] T.X.T. Sayle, S.C. Parker, C.R.A. Catlow, Surf. Sci. 316 (1994) 329–336.
[19] N.J. Lawrence, J.R. Brewer, L. Wang, T.-S. Wu, J. Wells-Kingsbury, M.M. Ihrig, G. Wang, Y.-L. Soo, W.-N. Mei, C.L. Cheung, Nano Lett. 11 (2011) 2666–2671.
[20] C.T. Campbell, C.H.F. Peden, Science 309 (2005) 713–714.
[21] J. Kaspar, P. Fornasiero, M. Graziani, Catal. Today 50 (1999) 285–298.
[22] S. Scire, S. Minico, C. Crisafulli, C. Satriano, A. Pistone, Appl. Catal., B 40 (2003) 43–49.
[23] D. Delimaris, T. Ioannides, Appl. Catal., B 89 (2009) 295–302.
[24] J.I. Gutierrez-Ortiz, B. de Rivas, R. Lopez-Fonseca, J.R. Gonzalez-Velasco, Appl. Catal., B 65 (2006) 191–200.
[25] S. Kumar, J. Huang, N. Abbassi-Ghadi, P. Spanel, D. Smith, G.B. Hanna, Anal. Chem. 85 (2013) 6121–6128.
[26] A. Cork, K.C. Park, Med. Vet. Entomol. 10 (1996) 269–276.
[27] P. Martinez-Lozano, L. Zingaro, A. Finiguerra, S. Cristoni, J. Breath Res. 5 (2011).
[28] D. Mohn, N. Doebelin, S. Tadier, R.E. Bernabei, N.A. Luechinger, W.J. Stark, M. Bohner, J. Mater. Chem. 21 (2011) 13963–13972.
[29] X.Z. Du, L. Dong, C. Li, Y.Q. Liang, Y. Chen, Langmuir 15 (1999) 1693–1697.
[30] K. Motzfeldt, J. Phys. Chem. 59 (1955) 139–147.
[31] A.E. Newkirk, I. Aliferis, Anal. Chem. 30 (1958) 982–984.
[32] C. Binet, A. Badri, M. Boutonnetkizling, J.C. Lavalley, J. Chem. Soc., Faraday Trans. 90 (1994) 1023–1028.
[33] C. Binet, A. Badri, J.C. Lavalley, J. Phys. Chem. 98 (1994) 6392–6398.
[34] G. Finos, S. Collins, G. Blanco, E. del Rio, J. Maria Cies, S. Bernal, A. Bonivardi, Catal. Today 180 (2012) 9–18.
[35] M.L. Dos Santos, R.C. Lima, C.S. Riccardi, R.L. Tranquilin, P.R. Bueno, J.A. Varela, E. Longo, Mater. Lett. 62 (2008) 4509–4511.
[36] E.M. Koeck, M. Kogler, T. Bielz, B. Kloetzer, S. Penner, J. Phys. Chem. C 117 (2013) 17666–17673.
[37] C.K. Huang, P.F. Kerr, Am. Mineral. 45 (1960) 311–324.
[38] L. Torrente-Murciano, A. Gilbank, B. Puertolas, T. Garcia, B. Solsona, D. Chadwick, Appl. Catal., B 132 (2013) 116–122.
[39] N. Yi, R. Si, H. Saltsburg, M. Flytzani-Stephanopoulos, Appl. Catal., B 95 (2010) 87–92.
[40] F.M.Z. Zotin, L. Tournayan, J. Varloud, V. Perrichon, R. Frety, Appl. Catal., A 98 (1993) 99–114.
[41] M. Breysse, J. Veron, B. Claudel, LatreillH., M. Guenin, J. Catal. 27 (1972) 275–280.